PHYSICAL REVIEW D **85,** 043506 (2012)

Observational constraints on the averaged universe

Chris Clarkson,[1] Timothy Clifton,[2] Alan Coley,[3] and Rockhee Sung[1]

[1]*Astrophysics, Cosmology, and Gravity Center, and Department of Mathematics and Applied Mathematics, University of Cape Town, South Africa*

[2]*Department of Astrophysics, University of Oxford, United Kingdom*

[3]*Department of Mathematics and Statistics, Dalhousie University, Halifax, Canada*

(Received 9 November 2011; published 7 February 2012; publisher error corrected 14 August 2014)

Averaging in general relativity is a complicated operation, due to the general covariance of the theory and the nonlinearity of Einstein's equations. The latter of these ensures that smoothing spacetime over cosmological scales does not yield the same result as solving Einstein's equations with a smooth matter distribution, and that the smooth models we fit to observations need not be simply related to the actual geometry of spacetime. One specific consequence of this is a decoupling of the geometrical spatial curvature term in the metric from the dynamical spatial curvature in the Friedmann equation. Here we investigate the consequences of this decoupling by fitting to a combination of Hubble Space Telescope (HST), CMB, type Ia supernovae (SNIa), and baryon acoustic oscillation (BAO) data sets. We find that only the geometrical spatial curvature is tightly constrained and that our ability to constrain dark energy dynamics will be severely impaired until we gain a thorough understanding of the averaging problem in cosmology.

DOI: 10.1103/PhysRevD.85.043506 PACS numbers: 98.80.Es

I. INTRODUCTION

The standard model of cosmology relies on the assumption that the Universe is well described at all points in space and time by a single linearly perturbed Friedmann-Lemaître-Robertson-Walker (FLRW) geometry (except in the vicinity of black holes and neutron stars), and that this geometry obeys Einstein's equations. However, in an inhomogeneous universe this is almost certainly not true. Even if the gravitational interaction behaves exactly as Einstein predicted on small scales, this will not be true for large-scale averages. A critical problem in cosmology is therefore determining the form of deviations from Einstein's equations when considering geometry averaged on large scales and what the effects of these deviations will be on observations (for a review, see [1]). This has been the subject of some controversy, with opinions ranging from the suggestion that the effects of averaging could completely explain the recently observed accelerating expansion of the Universe without the need for any dark energy [2–9], to the claim that it is completely negligible [10–21]. Others suggest that while the effects of averaging may not be responsible for the apparent acceleration, they may be important for precision cosmology [22–32].

In this paper we take the solutions to the field equations derived from using an exact and fully covariant averaging procedure and compare them to observations. These solutions have decoupled spatial curvature parameters in the metric and the Friedmann equation, and reduce to the FLRW solutions of Einstein's equations when these parameters are equal. We find that the constraints available on the spatial curvature parameter appearing in the Friedmann equation are considerably weaker than those available on the spatial curvature parameter appearing in the macroscopic metric. In particular, the constraints from the CMB are considerably weakened and no longer signal a flat universe. This allows for the possibility of averaging having non-negligible dynamical consequences. We also find that some data sets prefer models in which the two curvature parameters are not equal.

II. SPACETIME AVERAGING AND MACROSCOPIC GRAVITY

There are a number of averaging procedures that have been introduced in order to study the large-scale evolution of inhomogeneous spacetimes. An exact and covariant approach that allows tensor quantities to be averaged, as well as scalars, was provided by Zalaletdinov [33]. Here the geometric objects that exist on the spacetime manifold are averaged, and the field equations that these quantities satisfy are constructed. This is achieved using bilocal averaging operators over closed regions of spacetime, Σ, that contain the supporting points x (see [33]). The result of averaging X is then denoted by $\langle X\rangle$.

By using this definition we can now consider the average of various geometric objects. Following Zalaletdinov, we denote the average of the connection as $\langle\Gamma^{\mu}{}_{\nu\rho}\rangle$, and define a new macroscopic Riemann tensor

$$M^{\mu}{}_{\nu\alpha\beta} = \partial_{\alpha}\langle\Gamma^{\mu}{}_{\nu\beta}\rangle - \partial_{\beta}\langle\Gamma^{\mu}{}_{\nu\alpha}\rangle + \langle\Gamma^{\mu}{}_{\sigma\alpha}\rangle\langle\Gamma^{\sigma}{}_{\nu\beta}\rangle - \langle\Gamma^{\mu}{}_{\sigma\beta}\rangle\langle\Gamma^{\sigma}{}_{\nu\alpha}\rangle. \tag{1}$$

Crucially, $M^{\mu}{}_{\nu\alpha\beta} \neq \langle R^{\mu}{}_{\nu\alpha\beta}\rangle$, where $\langle R^{\mu}{}_{\nu\rho\sigma}\rangle$ is the average of the microscopic Riemann tensor. From these quantities one can then construct the macroscopic field equations [33]:

$$\langle g^{\beta\epsilon}\rangle M_{\gamma\beta} - \tfrac{1}{2}\delta^{\epsilon}{}_{\gamma}\langle g^{\mu\nu}\rangle M_{\mu\nu} = 8\pi G\langle T^{\epsilon}{}_{\gamma}\rangle + \langle g^{\mu\nu}\rangle\Big(Z^{\epsilon}{}_{\mu\nu\gamma} - \tfrac{1}{2}\delta^{\epsilon}{}_{\gamma}Z^{\alpha}{}_{\mu\nu\alpha}\Big), \tag{2}$$

where $\langle T^{\epsilon}{}_{\gamma}\rangle$ is the averaged energy-momentum tensor, $\langle g_{\mu\nu}\rangle$ is the averaged metric, and $Z^{\alpha}{}_{\mu\nu\beta} = 2Z^{\alpha}{}_{\mu[\epsilon\underline{\nu}\beta]}{}^{\epsilon}$ is a correlation tensor defined by

$$Z^{\alpha}{}_{\beta[\gamma}{}^{\mu}{}_{\underline{\nu}\sigma]} = \langle\Gamma^{\alpha}{}_{\beta[\gamma}\Gamma^{\mu}{}_{\underline{\nu}\sigma]}\rangle - \langle\Gamma^{\alpha}{}_{\beta[\gamma}\rangle\langle\Gamma^{\mu}{}_{\underline{\nu}\sigma]}\rangle, \tag{3}$$

where underlined indices are not included in antisymmetrization. This quantity must obey the differential constraint $Z^{\alpha}{}_{\beta[\gamma}{}^{\mu}{}_{\underline{\nu}\sigma;\lambda]} = 0$, where the covariant derivative here is defined using the averaged connection $\langle\Gamma^{\mu}{}_{\nu\rho}\rangle$. The macroscopic field equations (2) replace Einstein's equations on large scales.

A. Macroscopic FLRW solutions

The solutions to the macroscopic field equations (2), with a FLRW ansatz for the macroscopic metric, have recently been studied in [24,34–37], where it was found that the extra terms involving the correlation tensor $Z^{\alpha}{}_{\beta[\gamma}{}^{\mu}{}_{\underline{\nu}\sigma]}$ take the same form in the macroscopic field equations that a spatial curvature term takes in Einstein's equations. In fact, for a spatially flat macroscopic metric with spatial correlations only, it can be shown that extra terms in Eq. (2) can *only* take the form of spatial curvature. Any other form would be incompatible with either the conservation equations, their integrability conditions, or the algebraic constraints that $Z^{\alpha}{}_{\beta[\gamma}{}^{\mu}{}_{\underline{\nu}\sigma]}$ must satisfy for consistency of the averaging scheme. Thus, the averaged Einstein field equations for a spatially flat, homogeneous, and isotropic macroscopic spacetime geometry take the form of the Friedmann equations of general relativity for a nonflat FLRW geometry. That is, the spatial curvature of the macroscopic spacetime is decoupled from the spatial curvature that appears in the macroscopic Friedmann equation. This is an important difference from the standard approach to cosmology, where it is assumed that Einstein's field equations are valid whatever the smoothing scale and that the spatial curvature in the Friedmann equation is therefore identical to the spatial curvature of the macroscopic spacetime.

Using the results above we motivate the following phenomenological cosmological model. We write the line element of the macroscopic geometry as

$$ds^2 = \langle g_{\mu\nu}\rangle dx^{\mu}dx^{\nu} = -dt^2 + a^2(t)\left[\frac{dr^2}{1-k_{\rm g}r^2} + r^2 d\Omega\right], \tag{4}$$

where the geometrical curvature, $k_{\rm g}$, is, in general, a function of the scale of Σ. The scale factor $a(t)$ is that of the macroscopic spacetime. On scales larger than Σ the macroscopic field equations, (2), then become

$$H^2 = \frac{\dot{a}^2}{a^2} = \frac{8\pi G}{3}\rho - \frac{k_{\rm d}}{a^2} + \frac{\Lambda}{3}, \tag{5}$$

where the "dynamical curvature," $k_{\rm d}$, is again a function of scale, and we have included in $k_{\rm d}$ here contributions from both the spatial curvature in the metric, $k_{\rm g}$, and the terms in Eq. (2) that involve the correlation tensor, $Z^{\alpha}{}_{\beta[\gamma}{}^{\mu}{}_{\underline{\nu}\sigma]}$. Only if the contribution from $Z^{\alpha}{}_{\beta[\gamma}{}^{\mu}{}_{\underline{\nu}\sigma]}$ vanishes do we recover the usual result $k_{\rm g} = k_{\rm d}$, and even in this case we can still have a scale dependence. Generally, in spacetimes that are inhomogeneous on small scales we do not expect these two "spatial curvature" terms to be equal. Defining $\Omega_{k_{\rm g}} = -k_{\rm g}/a_0^2H_0^2$ and $\Omega_{k_{\rm d}} = -k_{\rm d}/a_0^2H_0^2$ the macroscopic Friedmann equation then becomes $1 = \Omega_m + \Omega_{k_{\rm d}} + \Omega_{\Lambda}$, where Ω_m and Ω_{Λ} are the usual expressions for the fraction of the energy content of the Universe in matter and the cosmological constant, respectively. Note that Ω_{Λ} is a function of smoothing scale, whereas Λ is not. The quantity $\Omega_{k_{\rm g}}$ does not have to satisfy a constraint of this kind as it is now decoupled from the Friedmann equation. Thus, we arrive at a parametrized phenomenological model within which we can analyze data in order to study the potential observational effects of averaging.

B. Observables in the macroscopic universe

We will now consider distance-redshift relations in the FLRW solutions of macroscopic gravity. These provide the basis for many key observational tests of the cosmological background.

First, we need to know the trajectories of photons in the macroscopic geometry. We will take these as null trajectories with respect to the macroscopic metric that has been constructed to approximate the distance between two points in spacetime separated by scales above that of Σ. We consider this to be a reasonable assumption for the average of a large number of photon trajectories, but note that it will not be true for each individual null curve of the microscopic spacetime. If this assumption is wrong then it could lead to profound differences with the results of applying Einstein's equations directly to nonlocal averaged quantities [38,39]. Our approach should therefore be considered a conservative one.

Let us now derive the luminosity distance-redshift relation in the macroscopic geometry. Integrating a null trajectory in the geometry (4), assuming $\Omega_{k_{\rm g}}$ and $\Omega_{k_{\rm d}}$ are constant, and using the solutions to the macroscopic Friedmann equation (5), gives

$$d_L(z) = \frac{(1+z)}{H_0\sqrt{|\Omega_{k_{\rm g}}|}} f_{k_{\rm g}}\left(\int_{(1/1+z)}^{1}\frac{\sqrt{|\Omega_{k_{\rm g}}|}da}{\sqrt{\Omega_{k_{\rm d}}a^2 + \Omega_{\Lambda}a^4 + \Omega_m a}}\right), \tag{6}$$

where $f_{k_g}(x) = \sinh(x)$, x or $\sin(x)$ when $k_g < 0$, $k_g = 0$ or $k_g > 0$, respectively. This expression reduces to the usual one when $\Omega_{k_g} = \Omega_{k_d}$.

III. DATA ANALYSIS

We can now compare our averaged models to various cosmological probes.

Hubble rate.—A vital tool for constraining dark energy is the local Hubble rate. We use Hubble rate data from HST measurements [40], which give $H_0 = 74.2 \pm 3.6\ \mathrm{km\,s^{-1}\,Mpc^{-1}}$, and we assume Gaussian errors.

Cosmic microwave background.—The CMB is well known to tightly constrain spatial curvature in the standard cosmology. When $\Omega_{k_g} = \Omega_{k_d}$ constraints from the WMAP 7 yr data release [41], combined with HST [40] and BAO data [42], gives $-0.0133 < \Omega_k < 0.0084$ (95% confidence limit). Principally, this constraint arises from the tight bounds on the area distance to the surface of last scattering, which must be $(1 + z_*)d_A(z_*) = 14150 \pm 150$ Mpc. We fit three parameters which are predicted by the model: The decoupling epoch (z_*), the acoustic scale (l_A), and the shift parameter (R), which are sufficient to capture the constraints from the CMB [41]. To obtain likelihoods, we also use the inverse covariance matrix for the WMAP distance priors for these parameters, as given in Table 10 from [41].

Supernovae.—Another key probe of the large-scale expansion of the Universe is the observation of SNIa. These events are considered to be "standardizable candles," in that their absolute magnitude can be approximated when "stretch" and "color" parameters have been extracted from fits to light-curve templates. They allow the expansion history of the Universe to be mapped and are widely considered to be one of the most compelling sources of evidence for the existence of dark energy. Therefore, we consider them here in the context of the FLRW solutions to macroscopic gravity in order to determine the consequences of allowing $\Omega_{k_g} \neq \Omega_{k_d}$. The supernova data used in obtaining these constraints are the Union2 data sets [43] and the Sloan Digital Sky Survey (SDSS) data sets [44].

Baryon acoustic oscillations.—Observations of BAOs provide a direct measurement of the Hubble rate at nonzero redshifts and are therefore a powerful tool for constraining dark energy. However, the interpretation of BAOs relies on assumptions about the evolution of structure in the Universe that may not be valid if averaging is important. Therefore, we choose to use BAO data only sparingly. We use the fraction of the comoving sound horizon to volume distance for the two points at redshifts $z = 0.2$ and 0.35. The inverse covariance matrix is given by Eq. 5 from [42].

A. Parameter constraints

We use the Monte Carlo Markov Chain (MCMC) method to obtain the marginalized errors on the model parameters from the likelihood function by using the publicly available package COSMOMC [45].

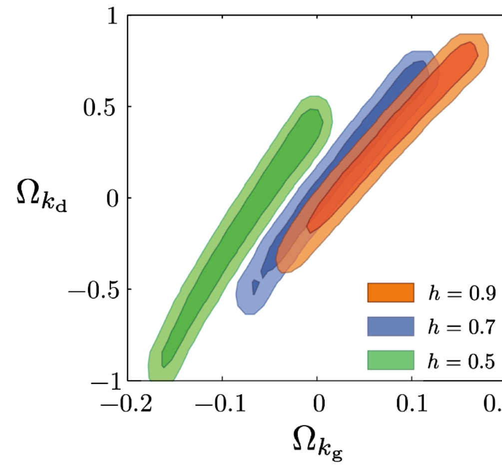

FIG. 1 (color online). Constraints on Ω_{k_g} and Ω_{k_d} from the CMB for $H_0 = 50$, 70 and 90 $\mathrm{km\,s^{-1}\,Mpc^{-1}}$, with the other parameters marginalized over. Shaded areas are 68% and 95% confidence regions.

First, consider CMB + H_0 constraints, as these lead to extremely tight constraints on spatial curvature in the standard model. It can be seen from Fig. 1 that when $\Omega_{k_g} \neq \Omega_{k_d}$ the CMB + H_0 no longer constrains spatial curvature significantly, principally due to a degeneracy between the effects of Ω_{k_g} and Ω_{k_d} in Eq. (6). In fact, even with $\Lambda = 0$ there exist values of k_g and k_d that satisfy the observations. These results significantly weaken a key part of the evidence for both a spatially flat universe and a nonzero value of Λ.

In Fig. 2 we show the combined constraints that can be imposed on Ω_{k_g} and Ω_{k_d} using data from the HST, the WMAP 7 yr data of the temperature-temperature correlations in the CMB, the Union 2 and SDSS SNIa data sets, and the constraints on the "volume distance" from the BAOs. Figure 3 shows the constraints available on Ω_m and Ω_Λ from the same data sets.

It is clear that the effect of allowing Ω_{k_g} and Ω_{k_d} to be independent has considerable consequences for these probability distributions. The marginalized posterior values of each parameter in the various cases are given in Table I. These values differ considerably from the case where $\Omega_{k_g} = \Omega_{k_d}$, which are shown in the same table for comparison. It can be seen that the additional freedom gained by allowing $\Omega_{k_g} \neq \Omega_{k_d}$ is considerable, with constraints on Ω_Λ and the two Ω_k being significantly weaker than in the standard approach. The combination of all of these observables, however, still appears to provide strong evidence for the existence of dark energy and is still consistent with a spatially flat universe. Nevertheless, it is striking that constraints on Ω_{k_g} are an order of magnitude tighter than those on Ω_{k_d}.

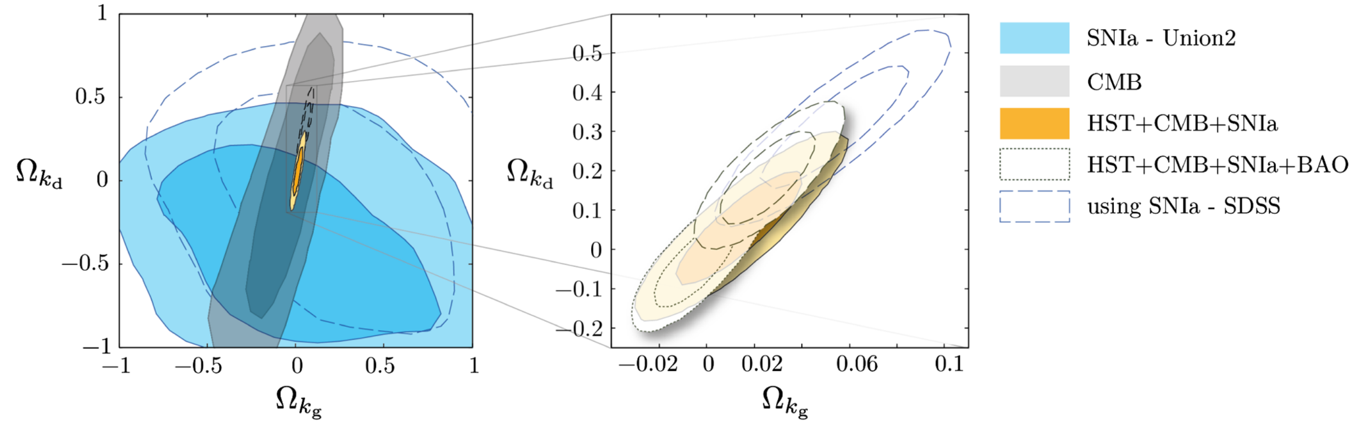

FIG. 2 (color online). Constraints on the two curvature parameters from different data sets. In the left panel we show the constraints from the CMB (the filled, thin, central contours) and SNIa (the filled, wide contours at the bottom of the plot for Union2, and unfilled and dashed for SDSS) separately, as well as the combined constraints including HST. In the right panel we show the combined constraints, with the smaller lightly shaded regions in the foreground now including the BAO. The constraints from the CMB and SNIa are extremely weak individually, but tighten when combined with HST data. Note that only the geometrical curvature is tightly constrained and not the dynamical one. The SDSS SNIa data can also be seen as inconsistent with $\Omega_{k_g} = 0$ at greater than 95% confidence.

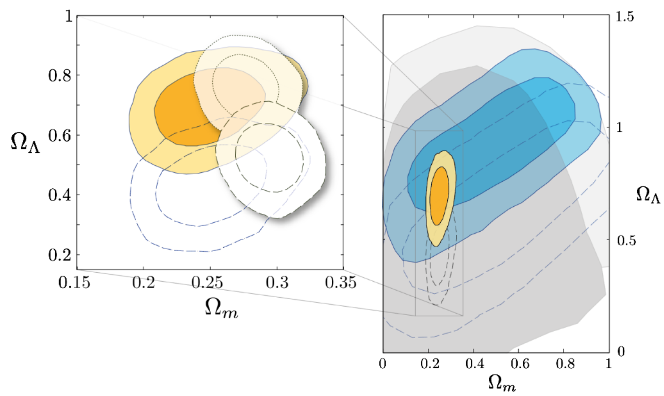

FIG. 3 (color online). Constraints on Ω_m and Ω_Λ for the same data set combinations as in Fig. 2. The constraints from the CMB and SNIa separately are again much weaker here than in the standard case. In particular, $\Lambda = 0$ is consistent with the CMB data for any Ω_m. Union2 SNIa data, however, still clearly give $\Lambda \neq 0$. (For a discussion of bias see Ref. [56].)

B. Constraints on dark energy dynamics

Decoupling the geometrical and dynamical spatial curvature parameters does not appear to allow enough freedom to entirely account for the dark energy component (which is now signaled almost entirely by supernova observations rather than by both CMB + H_0 and SNIa observations as in the standard model). Nonetheless, considering averaged spacetimes considerably weakens our ability to constrain dark energy in a meaningful way. For example, if we parametrize the equation of state for dark energy as $w(z) = w_0 + w_a(1 - a) = w_0 + w_a z/(1 + z)$ then CMB + HST + BAO + SNIa(union2) gives only the weak constraint $w_0 = -1.612^{+0.511}_{-0.524}$, with almost no meaningful constraints on w_a at all. This can be compared with $w_0 = -1.066^{+0.202}_{-0.197}$ and $w_a = -0.130^{+1.141}_{-1.135}$ when $k_g = k_d$, as in Fig. 4. Clearly, the uncertainty arising from the averaging problem is hugely amplified when we try to constrain the dynamical properties of dark energy.

TABLE I. Constraints on curvature and Λ with decoupled curvature parameters and in the standard model.

Data sets	Ω_{k_d}	Ω_{k_g}	Ω_Λ	$\Omega_{k_d} = \Omega_{k_g}$	Ω_Λ
CMB	$-0.053^{+0.152}_{-0.153}$	$-0.036^{+0.562}_{-0.572}$	$+0.525^{+0.417}_{-0.524}$	$-0.069^{+0.109}_{-0.112}$	$+0.548^{+0.331}_{-0.303}$
CMB + HST	$+0.036^{+0.062}_{-0.064}$	$+0.185^{+0.396}_{-0.415}$	$+0.564^{+0.415}_{-0.401}$	$+0.006^{+0.007}_{-0.007}$	$+0.746^{+0.023}_{-0.023}$
SNIa (Union2)	$+0.012^{+0.513}_{-0.485}$	$-0.369^{+0.398}_{-0.410}$	$+0.902^{+0.189}_{-0.187}$	$-0.205^{+0.285}_{-0.282}$	$+0.858^{+0.192}_{-0.194}$
SNIa (SDSS)	$+0.233^{+0.466}_{-0.451}$	$-0.173^{+0.492}_{-0.507}$	$+0.641^{+0.230}_{-0.225}$	$+0.073^{+0.301}_{-0.298}$	$+0.547^{+0.203}_{-0.204}$
CMB + HST + SNIa(union2)	$+0.014^{+0.017}_{-0.017}$	$+0.055^{+0.092}_{-0.092}$	$+0.695^{+0.080}_{-0.082}$	$+0.005^{+0.007}_{-0.007}$	$+0.739^{+0.020}_{-0.021}$
CMB + HST + SNIa(SDSS)	$+0.054^{+0.020}_{-0.020}$	$+0.311^{+0.100}_{-0.101}$	$+0.436^{+0.087}_{-0.089}$	$-0.004^{+0.009}_{-0.009}$	$+0.685^{+0.024}_{-0.024}$
CMB + HST + SNIa(union2) + BAO	$-0.004^{+0.011}_{-0.011}$	$-0.033^{+0.070}_{-0.069}$	$+0.755^{+0.068}_{-0.070}$	$+0.000^{+0.006}_{-0.006}$	$+0.723^{+0.016}_{-0.016}$
CMB + HST + SNIa(SDSS) + BAO	$+0.026^{+0.012}_{-0.012}$	$+0.183^{+0.072}_{-0.070}$	$+0.522^{+0.070}_{-0.073}$	$+0.001^{+0.007}_{-0.006}$	$+0.698^{+0.017}_{-0.017}$

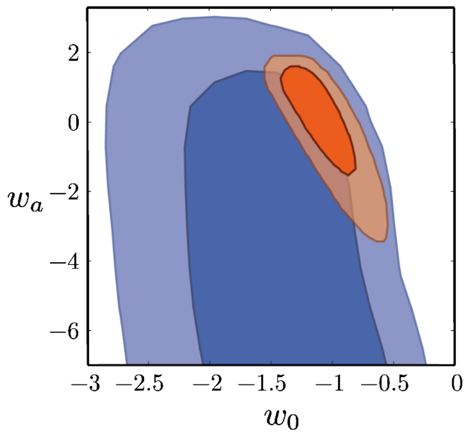

FIG. 4 (color online). Marginalized constraints on the dark energy parameters, with (the small, filled region at the top right) and without (the large, filled region that occupies most of the plot) assuming $k_g = k_d$. Allowing for effects due to averaging removes our ability to constrain the possible evolution of the dark energy equation of state.

C. Scale dependent curvature parameters

As well as k_g and k_d being allowed to be different, a second consequence of using an averaged geometry is that these parameters could become scale dependent. This possibility introduces a considerable amount of extra freedom and hence we consider it separately here from the more restricted case we have considered so far (where k_g and k_d are different, but scale independent).

The cosmological probes we have discussed all make observations over different scales. The scale of BAOs at the present time is about 150 Mpc. High redshift SNIa (out to $z \sim 1$) cover a range of scales out to several Gpc while the CMB involves making observations on the scale of the horizon ($\sim$ 14 Gpc). By introducing a scale dependence into k_g and k_d we can therefore potentially reintroduce the effects of spatial curvature on the scales of SNIa and BAOs, while still satisfying the stringent constraints available on the largest scales from the CMB. The question then becomes whether or not it is possible for observations to effectively constrain spatial curvature on different scales in the Universe. A positive detection of conflicting measurements of spatial curvature on different length scales would be a sure sign of nontrivial averaging effects [9,26].

As we have shown, the CMB may no longer imply spatial flatness or a nonzero Ω_Λ at all (see Fig. 1). If spatial curvature on the scale of SNIa observations is allowed to be independent from the constraints imposed by other observables, then the evidence available for the existence of a nonzero Ω_Λ is again severely weakened (see Fig. 3). Also, if Ω_{k_g} and Ω_{k_d} vary with sufficient rapidity on scales of interest for SNIa observations then we can no longer treat them as being simple constants when analyzing the data. Instead, since we average these observables over the sky, what we are doing is effectively averaging the geometry out to some redshift. This should be expected to result in redshift dependent effective curvature parameters, and in this case one could end up with curvature parameters that are effectively functions of radial distance, $k = k(r)$.

This picture is somewhat similar to Lemaître-Tolman-Bondi void models of the Universe, where the Earth is at the center of a large spherically symmetric inhomogeneity. It is well known that such models are able to explain the supernova data without evoking the existence of dark energy [46], but at the expense of strongly violating the Copernican principle. In the present interpretation no such violation need occur, as *all* observers will experience a universe with $k = k(r)$, with themselves at the center of symmetry. This would relieve the key philosophical problem associated with these models as an explanation of the data. It would also relieve the strong constraints on these models that are available from the kinematic Sunyaev-Zeldovich effect [47–49], as every cluster would experience (approximately) isotropic CMB radiation, just as we do on Earth. However, such a departure from the usual interpretation of Lemaître-Tolman-Bondi models would also undoubtedly require revisiting the problem, as the field equations would be modified by additional terms due to averaging and cannot just be considered as the normal Einstein field equations as has been the case so far. In particular, the relation between averaging observables on the sky and averaging the field equations spatially is nontrivial, and extending our ansatz given by Eqs. (4) and (5) to the spherically symmetric case may not be obvious.

IV. CONCLUSIONS

We have presented and constrained models of the large-scale Universe that result from averaging the geometry of spacetime. These models have decoupled spatial curvature parameters in the macroscopic line element (Ω_{k_g}) and the Friedmann equation (Ω_{k_d}), and provide a qualitative alternative to the standard model of cosmology. Therefore, they can be used to analyze the statistical significance of the standard model in a larger space of models that allows for some of the nontrivial consequences of averaging.

By using HST, CMB, BAO, and SNIa data it is clear that the effect of allowing Ω_{k_g} and Ω_{k_d} to be independent has considerable consequences for parameter estimation. Analysis of the available data shows that the size of the 68% and 95% confidence regions of Ω_Λ, Ω_{k_g}, and Ω_{k_d} are all much larger than in the standard model. There are even tantalizing hints that the data may favor $\Omega_{k_g} \neq \Omega_{k_d}$ (the combination of HST, CMB, and SDSS SNIa data excludes $\Omega_{k_g} = \Omega_{k_d}$ at the 95% confidence level). However, while the evidence for $\Omega_\Lambda \neq 0$ available from individual observables can be considerably reduced, the combination of SN, CMB, HST, and BAO data still provides strong evidence for the existence of dark energy, as long as Ω_{k_g} and Ω_{k_d} are scale independent universal constants. Relaxing this last assumption makes combining observables on different scales a much more complicated problem, and it is highly probable that such additional freedom will significantly weaken the evidence for $\Omega_\Lambda \neq 0$.

The way that this situation should be modeled and constrained with data is still an open problem. Relating observables to spatial averages is known to be nontrivial, and is sometimes described as ‘‘dressing’’ the cosmological parameters [50–52]. Although our ansatz given by Eqs. (4) and (5) is well motivated by macroscopic gravity, other averaging schemes can be used to motivate other phenomenological models, such as in [9] where Buchert's scheme was used to motivate a time-dependent curvature parameter. Other ways of relating average quantities to observables also exist [53–55], and different observational constraints arise depending on the method used. It remains an open problem to decide on the ‘‘correct’’ way to go about this.

Finally, we have shown that introducing uncertainty due to averaging into our models of the Universe dramatically weakens the constraints that can be imposed on the equation of state of dark energy, and we expect this result to be robust to the averaging scheme used. As a consequence, it is therefore necessary to understand and incorporate the effects of averaging in general relativity into our models if we are to begin attempting precision cosmology.

ACKNOWLEDGMENTS

T. C. acknowledges the support of the STFC and the BIPAC, A. C. acknowledges the support of the NSERC, and R. S. and C. C. acknowledge funding from the NRF (South Africa). Numerical analysis was performed using facilities at the Centre for High Performance Computing, South Africa.

[1] C. Clarkson, G. Ellis, J. Larena, and O. Umeh, Rep. Prog. Phys. **74**, 112901 (2011).
[2] T. Buchert, Gen. Relativ. Gravit. **32**, 105 (2000).
[3] T. Buchert, Gen. Relativ. Gravit. **33**, 1381 (2001).
[4] S. Rasanen, J. Cosmol. Astropart. Phys. 02 (2004) 003.
[5] E. Barausse, S. Matarrese, and A. Riotto, Phys. Rev. D **71**, 063537 (2005).
[6] E. W. Kolb, S. Matarrese, and A. Riotto, New J. Phys. **8**, 322 (2006).
[7] S. Rasanen, J. Cosmol. Astropart. Phys. 11 (2006) 003.
[8] M. Kasai, Prog. Theor. Phys. **117**, 1067 (2007).
[9] J. Larena, J. M. Alimi, T. Buchert, M. Kunz, and P. -S. Corasaniti, Phys. Rev. D **79**, 083011 (2009).
[10] A. Ishibashi and R. M. Wald, Classical Quantum Gravity **23**, 235 (2006).
[11] E. E. Flanagan, Phys. Rev. D **71**, 103521 (2005).
[12] C. M. Hirata and U. Seljak, Phys. Rev. D **72**, 083501 (2005).
[13] G. Geshnizjani, D. J. H. Chung, and N. Afshordi, Phys. Rev. D **72**, 023517 (2005).
[14] C. Bonvin, R. Durrer, and M. Gasperini, Phys. Rev. D **73**, 023523 (2006).
[15] C. Bonvin, R. Durrer, and M. Kunz, Phys. Rev. Lett. **96**, 191302 (2006).
[16] J. Behrend, I. A. Brown, and G. Robbers, J. Cosmol. Astropart. Phys. 01 (2008) 013.
[17] N. Kumar and E. E. Flanagan, Phys. Rev. D **78**, 063537 (2008).
[18] A. Krasinski, C. Hellaby, M.-N. Celerier, and K. Bolejko, Gen. Relativ. Gravit. **42**, 2453 (2010).
[19] K. Tomita, in *Report of the KEK Cosmophysics Workshop DE2008* (Institute of High Energy Physics, Tsukuba, 2008).
[20] D. Baumann, A. Nicolis, L. Senatore, and M. Zaldarriaga, arXiv:1004.2488.
[21] S. R. Green and R. M. Wald, Phys. Rev. D **83**, 084020 (2011).
[22] H. Russ, M. H. Soffel, M. Kasai, and G. Borner, Phys. Rev. D **56**, 2044 (1997).
[23] E. W. Kolb, S. Matarrese, A. Notari, and A. Riotto, Phys. Rev. D **71**, 023524 (2005).
[24] A. A. Coley, N. Pelavas, and R. M. Zalaletdinov, Phys. Rev. Lett. **95**, 151102 (2005).
[25] N. Li and D. J. Schwarz, Phys. Rev. D **76**, 083011 (2007).
[26] A. A. Coley, Classical Quantum Gravity **27**, 245017 (2010).
[27] N. Li and D. J. Schwarz, Phys. Rev. D **78**, 083531 (2008).
[28] N. Li, M. Seikel, and D. J. Schwarz, Fortschr. Phys. **56**, 465 (2008).
[29] C. Clarkson, K. Ananda, and J. Larena, Phys. Rev. D **80**, 083525 (2009).
[30] C. Clarkson, AIP Conf. Proc. **1241**, 784 (2010).
[31] H. Chung, arXiv:1009.1333.
[32] O. Umeh, J. Larena, and C. Clarkson, J. Cosmol. Astropart. Phys. 03 (2011) 029.
[33] R. M. Zalaletdinov, Gen. Relativ. Gravit. **24**, 1015 (1992); R. M. Zalaletdinov*ibid.* **25**, 673 (1993).
[34] A. A. Coley and N. Pelavas, Phys. Rev. D **74**, 087301 (2006).
[35] A. A. Coley and N. Pelavas, Phys. Rev. D **75**, 043506 (2007).
[36] R. J. van den Hoogen, J. Math. Phys. (N.Y.) **50**, 082503 (2009).
[37] R. J. van den Hoogen, AIP Conf. Proc. **1122**, 408 (2009).
[38] C. Clarkson, G. Ellis, A. Faltenbacher, R. Maartens, O. Umeh, and J. -P. Uzan, arXiv:1109.2484.
[39] T. Clifton, A. A. Coley, and R. J. van den Hoogen (unpublished).

[40] A. G. Riess, L. Macri, S. Casertano, M. Sosey, H. Lampeitl, H. C. Ferguson, A. V. Filippenko, S. W. Jha *et al.*, Astrophys. J. **699**, 539 (2009).
[41] E. Komatsu *et al.*, Astrophys. J. Suppl. Ser. **192**, 18 (2011).
[42] B. A. Reid *et al.*, Mon. Not. R. Astron. Soc. **401**, 2148 (2010).
[43] R. Amanullah *et al.*, Astrophys. J. **716**, 712 (2010).
[44] R. Kessler *et al.*, Astrophys. J. Suppl. Ser. **185**, 32 (2009).
[45] A. Lewis and S. Bridle, Phys. Rev. D **66**, 103511 (2002).
[46] M.-N. Célérier and J. Schneider, Phys. Lett. A **249**, 37 (1998).
[47] J. Goodman, Phys. Rev. D **52**, 1821 (1995).
[48] J. García-Bellido and T. Haugbølle, J. Cosmol. Astropart. Phys. 09 (2008) 016.
[49] P. Bull, T. Clifton, and P. G. Ferreira, Phys. Rev. D **85**, 024002 (2012).
[50] T. Buchert and M. Carfora, Classical Quantum Gravity **19**, 6109 (2002).
[51] T. Buchert and M. Carfora, Phys. Rev. Lett. **90**, 031101 (2003).
[52] D. L. Wiltshire, New J. Phys. **9**, 377 (2007).
[53] B. M. Leith, S. C. C. Ng, and D. L. Wiltshire, Astrophys. J. **672**, L91 (2008).
[54] D. L. Wiltshire, Phys. Rev. D **80**, 123512 (2009).
[55] A. Wiegand and T. Buchert, Phys. Rev. D **82**, 023523 (2010).
[56] One should bear in mind here that the Union2 data make use of the SALT light-curve fitter [57], which requires stretch and color parameters to be extracted from the model that is being fitted, as well as the "intrinsic error." For the case of the Union2 data these parameters are taken from fitting to the ΛCDM model, such that $\chi^2_{\mathrm{reduced}} = 1$. This clearly biases fits against alternative models, such as the one being considered here, although the consequences of this are generally thought to be small as long as the shape of the Hubble diagram is similar to that of ΛCDM (as is the case here). For an example of the effect this can have on models that are not similar to ΛCDM see, e.g., [58,59].
[57] J. Guy *et al.*, Astron. Astrophys. **466**, 11 (2007).
[58] T. Clifton, P. G. Ferreira, and K. Land, Phys. Rev. Lett. **101**, 131302 (2008).
[59] P. R. Smale and D. L. Wiltshire, Mon. Not. R. Astron. Soc. **413**, 367 (2011).